Semicond. Sci. Technol. **11** (1996) 1613–1617. Printed in the UK

Electrons in mesoscopically inhomogeneous magnetic fields

P D Ye†, D Weiss†‡, R R Gerhardts†, G Lütjering†, K von Klitzing† and H Nickel§

† Max-Planck-Institut für Festkörperforschung, D-70569 Stuttgart, Germany
‡ Experimentelle und Angewandte Physik, Universität Regensburg, D-93040 Regensburg, Germany
§ Forschungsinstitut der Deutschen Bundespost, D-64295 Darmstadt, Germany

Abstract. We investigated the low-field magnetoresistivity ρ_{xx} of a two-dimensional electron gas (2DEG) underneath microstructured ferromagnetic gratings. The strength and the direction of an externally applied magnetic field determines the strength and the shape of the micromagnet's stray field. Commensurability effects due to the imposed *periodic magnetic field* are in competition with similar effects resulting from a strain-induced *periodic electrostatic potential*, associated with the patterned ferromagnets on top of the heterojunction. The presence of both a periodic magnetic field and a periodic electrostatic potential gives rise to the interesting interference phenomena presented here.

By means of patterned ferromagnetic [1, 2] or superconducting [3] layers on top of two-dimensional electron systems, it is possible to study electron motion in inhomogeneous magnetic fields varying on a length scale small compared to the mean free path l_e of the electrons. By periodically arranging ferromagnetic 'wires' with submicron diameters on top of a high-mobility GaAs–AlGaAs heterojunction (figures 1(a, c)), it is possible, for example, to generate a one-dimensional (1D) periodic magnetic field in the plane of the two-dimensional electron gas (2DEG). In analogy, two-dimensional (2D) periodic or random magnetic fields can be generated by placing ferromagnetic dots either periodically ([4], see also figures 1(b, d)) or randomly on top of a 2DEG [5]. Here, we focus on transport properties of a 2DEG underneath ferromagnetic gratings (figures 1(a, c)) resulting in both a 1D periodic magnetic field and a 1D periodic electrostatic potential. The latter is due to different thermal expansion coefficients of the ferromagnetic material (here dysprosium) and the semiconductor layers, which gives rise to a strain-induced modulation of the kinetic energy of the electrons [6].

The effect of a weak periodic magnetic field on a 2DEG has been predicted to result in an oscillatory magnetoresistance, which reflects the commensurability between the period a of the magnetic field modulation and the classical cyclotron diameter $2R_c$ of the electrons at the Fermi energy E_F [7–10]. For a weak 1D magnetic modulation with modulation amplitude $|B_m|$ much smaller than the external magnetic field $|B_0|$, the magnetoresistance ρ_{xx} oscillates with minima appearing at magnetic fields given by [7–10]

$$2R_c = \frac{2\hbar k_F}{e|B_0|} = \left(\lambda + \frac{1}{4}\right) a \qquad (1)$$

where $\lambda = 0, 1, \ldots$ is an integer oscillation index, $k_F = \sqrt{2\pi n_s}$ is the Fermi wavenumber, n_s is the carrier density of the 2DEG, and a is the period of the 1D modulation in the x direction. This effect, observed recently [1–3], is intimately related to the commensurability (Weiss) oscillations observed in the resistivity ρ_{xx} of a 2DEG with weak electric modulation [11–13]. Similar to the electric case, the magnetic modulation modifies the energy spectrum [7–10]. The degenerate Landau levels are transformed into bands of finite width. The dispersion of these Landau bands provides an additional contribution to the resistivity ρ_{xx}, which vanishes only when the bandwidth becomes zero ('flat-band condition') [12, 13]. In contrast to equation (1), describing the flat-band condition for magnetic modulation, the flat-band condition for weak electrical modulation reads $2R_c = (\lambda - \frac{1}{4})a$ with $\lambda = 1, 2, \ldots$. Hence, ρ_{xx} of a 2DEG with a weak electric modulation displays minima at B_0 fields where maxima would appear in a weak magnetic modulation of the same period a.

For the case of a pure electric modulation, the additional contribution to ρ_{xx} has been related to the classical guiding centre drift of the cyclotron orbits, which vanishes if the flat-band condition holds [14]. This classical picture can be extended to include, in addition to an arbitrary periodic modulation $V_m(\boldsymbol{r}) = \sum_{q\neq 0} V_{\boldsymbol{q}} e^{i\boldsymbol{q}\boldsymbol{r}}$ of the electrostatic potential energy of an electron, a weak modulation $B_m(\boldsymbol{r}) = \sum_{q\neq 0} B_{\boldsymbol{q}} e^{i\boldsymbol{q}\boldsymbol{r}}$ of the z component of the magnetic field ($\boldsymbol{q} = (Kn_x, Kn_y)$ with $K = 2\pi/a$ and

0268-1242/96/111613+05$19.50

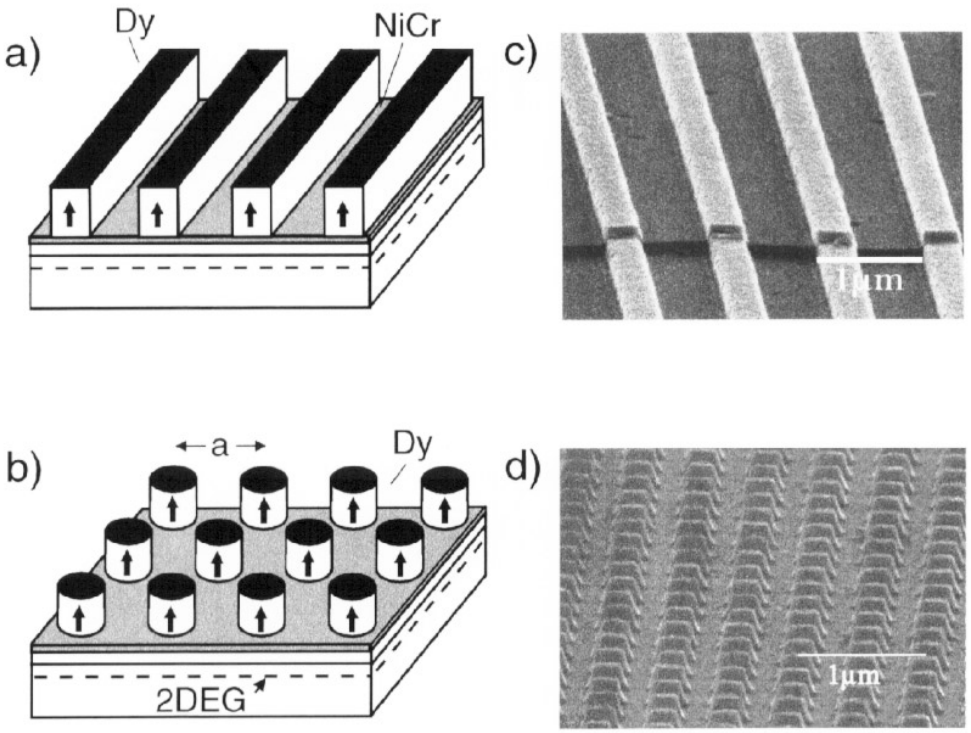

Figure 1. Sketch of ferromagnetic strips (a) and dots (b) used to generate a 1D and a 2D periodic magnetic field in the plane of a 2DEG in GaAs–AlGaAs heterojunctions. Arrows indicate a magnetization in the $\pm z$ direction. The corresponding electron micrographs show 200 nm high strips (c) and dots (d) made of dysprosium (Dy).

integers n_x, n_y, not simultaneously zero). Averaging the modulation-induced drift of the guiding centres over the unperturbed cyclotron orbits at field B_0 [14, 15], we obtain a change in the resistivity

$$\frac{\Delta\rho_{xx}}{\rho_0} = \frac{l_e^2}{2E_F^2}\sum_{q\neq 0} q_x^2|S|^2 \tag{2}$$

$$S \approx \left(\frac{2}{\pi q R_c}\right)^{1/2}\left[\sigma V_q \cos\left(qR_c - \frac{\pi}{4}\right) + \frac{k_F}{q}\hbar\omega_q \sin\left(qR_c - \frac{\pi}{4}\right)\right] \tag{3}$$

where $\rho_0 = 1/en_s\mu$ is the zero-field resistivity of the unmodulated 2DEG with the electron mobility μ, $\omega_q = eB_q/m^*$ (m^* is the effective electron mass of GaAs) and σ is either $+1$ or -1 depending on the direction of the externally applied magnetic field B_0. For our 1D modulation ($\boldsymbol{q} = (Kn_x, 0)$), we find $\Delta\rho_{xy} = \Delta\rho_{yx} = \Delta\rho_{yy} = 0$ to leading order in the small parameter $(\mu B)^{-1}$.

Our samples were prepared from high-mobility GaAs–AlGaAs heterojunctions. The 2DEG was located approximately 100 nm underneath the sample surface. The carrier density n_s and electron mobility μ at 4.2 K were $\sim 2.2 \times 10^{11}$ cm^{-2} and 1.3×10^6 cm^2 V^{-1} s^{-1} in the dark, corresponding to an elastic mean free path of ~ 10 μm. 50 μm wide Hall bars were fabricated by standard photolithographic techniques. Alloyed AuGe/Ni pads contact the 2DEG. A 10 nm thin NiCr film, evaporated on top of the devices, defines an equipotential plane to avoid electric modulation of the 2DEG. However, strain due to different thermal expansion coefficients of the ferromagnetic grating and the heterojunction always results in a weak electric periodic potential as the sample is cooled down to cryogenic temperatures. The Dy gratings with periods of 500 nm and 1 μm were defined by electron beam lithography on top of the NiCr gates. After developing the exposed PMMA resist, a 200 nm Dy film was evaporated. After lift-off in acetone, ferromagnetic gratings, like the one shown in figure 1(c), were obtained. Four-point resistance measurements were performed in a ^{4}He cryostat with superconducting coils using standard a.c. lock-in techniques.

Figure 2 displays the magnetoresistance of a 2DEG measured for different directions of the magnetization $\boldsymbol{M}$. The direction of $\boldsymbol{M}$ (see inset of figure 2) was adjusted by tilting the sample with respect to the direction of the external magnetic field which, in this case, was swept up to a maximum field of 10 T and then back to $B_0 = 0$ T. For the resistance measurements the samples were rotated back in such an orientation that the external magnetic field B_0 was applied normal to the plane of the 2DEG (z direction). Because the Dy microstructures used here show pronounced hard magnetic behaviour, the imposed magnetization is only slightly changed in the low-field region. If the strips are magnetized along their axis, essentially no magnetic modulation is imposed on the 2DEG, as expected, and the ρ_{xx} trace is virtually independent (on this scale) of the applied magnetic field. The situation changes dramatically if the strips are

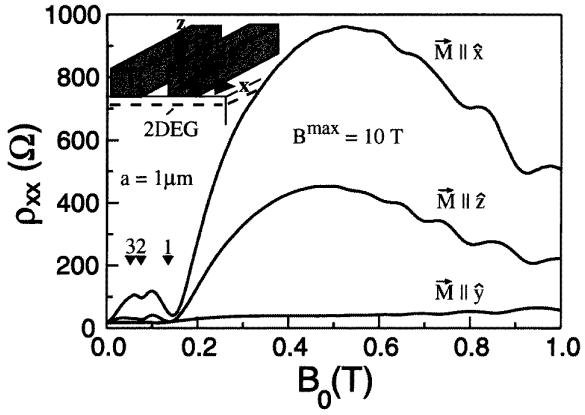

Figure 2. Resistance of a 2DEG as a function of the externally applied magnetic field B_0 (always pointing in the z direction) measured at 4.2 K. Different traces correspond to different directions of the magnetization M (see inset). The different amplitudes of the oscillations for $M \| \hat{x}$ and $M \| \hat{z}$ indicate different strengths of the stray field in the z direction and are probably a consequence of the rectangular shape of the wires (see figure 1(c)).

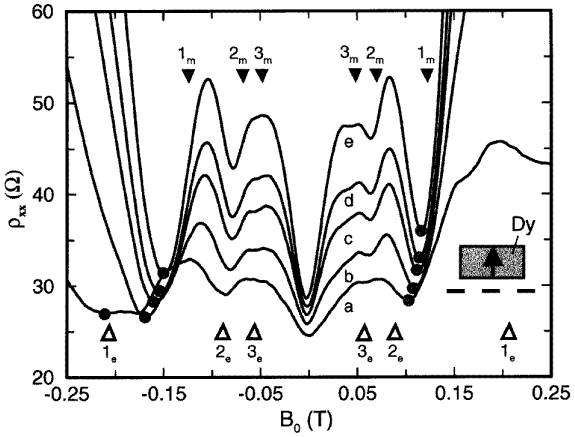

Figure 3. Low-field ρ_{xx} traces for a Dy grating with $a = 1$ μm taken at 4.2 K for $M \| \hat{z}$ (see inset) showing the shift of the ρ_{xx} minima with increasing B^{max}. Full triangles mark the position of the *magnetic* flat-band condition (subscript '*m*') while the open triangles mark the *electric* ones (subscript '*e*'). The full circles highlight the positions of the ρ_{xx} minima.

magnetized either in the z or in the x direction (see inset of figure 2). Pronounced oscillatory behaviour dominates ρ_{xx} with minima at magnetic field positions predicted for *pure* magnetic modulation. Hence, these traces display the *magnetic commensurability oscillations* anticipated by theory. Since on the other hand we know that a strain-induced electric modulation is present, we conclude that for the maximum 'conditioning' field of $B^{max} = 10$ T the strength of our micromagnets covers up the effect of the electrostatic potential modulation.

By increasing the magnetization M gradually starting from $M = 0$, the influence of both the electrostatic periodic potential and the magnetic modulation can clearly be seen [1]. This is shown in figure 3 for a magnetization of the strips in the z direction where the strain-induced electrostatic periodic potential is *in phase* (maxima of the periodic potential and the periodic magnetic field are both underneath the centres of the magnetic strips; see figure 5(c)) with the periodic magnetic field. In figure 3 traces labelled (a) to (e) are taken for different maximum 'conditioning' fields B^{max} between 1 T (a) and 10 T (e). With increasing B^{max} a richer oscillatory structure unfolds in ρ_{xx}, indicating a growing amplitude of the magnetic field modulation. Open triangles mark the expected positions of the minima (flat-band condition) for pure electric modulation at $2R_c = (\lambda - \frac{1}{4})a$ while filled ones mark pure magnetic modulation at $2R_c = (\lambda + \frac{1}{4})a$. With increasing strength of the magnets (corresponding to growing B_q in equation (3)) the minima position shift from electric-modulation-dominated minima to magnetic-modulation-dominated minima (from 2_e to 1_m for $B_0 > 0$ and from 1_e to 1_m for $B_0 < 0$). The asymmetry of the traces with respect to $B_0 = 0$ is a consequence of changing the sign of σ in equation (3) [1]. The shift of the minima in figure 3 corresponds to a growing magnetic contribution $s_m \equiv (k_F/q)\hbar\omega_q \sin\left(qR_c - \frac{\pi}{4}\right)$ in equation (3) whereas

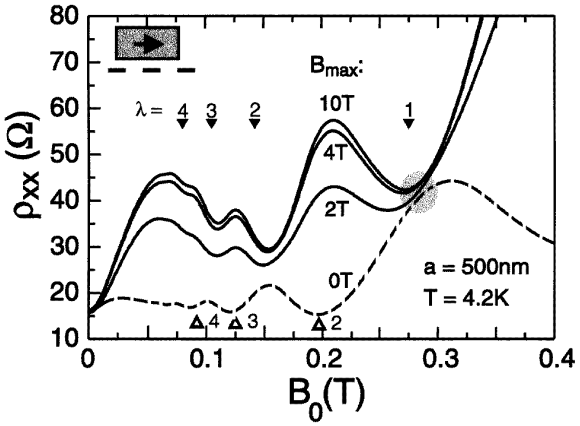

Figure 4. Low-field ρ_{xx} traces for a Dy grating with $a = 500$ nm measured at 4.2 K for $M \| \hat{x}$ (see inset). The dashed trace, taken after initial cooldown, reflects pure *electrostatic* commensurability oscillations. Solid traces are taken after magnetizing the wires (from $B^{max} = 2$ T to 10 T) in the x direction. Contributions to ρ_{xx} resulting from increased magnetic modulation simply add to the electrostatically induced ρ_{xx} changes. This is clearly visible at the magnetic flat-band condition $\lambda = 1$ where the resistance minima sit upon the maximum of the dashed trace.

the strain-induced contribution, $s_e \equiv V_q \cos\left(qR_c - \frac{\pi}{4}\right)$, is unaltered. The minima positions in ρ_{xx} are determined by the zeros of $|s_m + s_e|^2$. Hence, the shift can be used to estimate the amplitude of the magnetic stray field: assuming a simple sinusoidal modulation ($q = (2\pi/a, 0)$) we obtain a peak-to-peak modulation of 40 mT for trace (e) at $B_0 = 0$ [1].

The 'interference' of electric and magnetic modulation changes drastically if M is tilted in the x direction [15]. Now the magnetic modulation suffers a phase shift of $\pi/2$ with respect to the electric one (see figure 5(a)). Such a

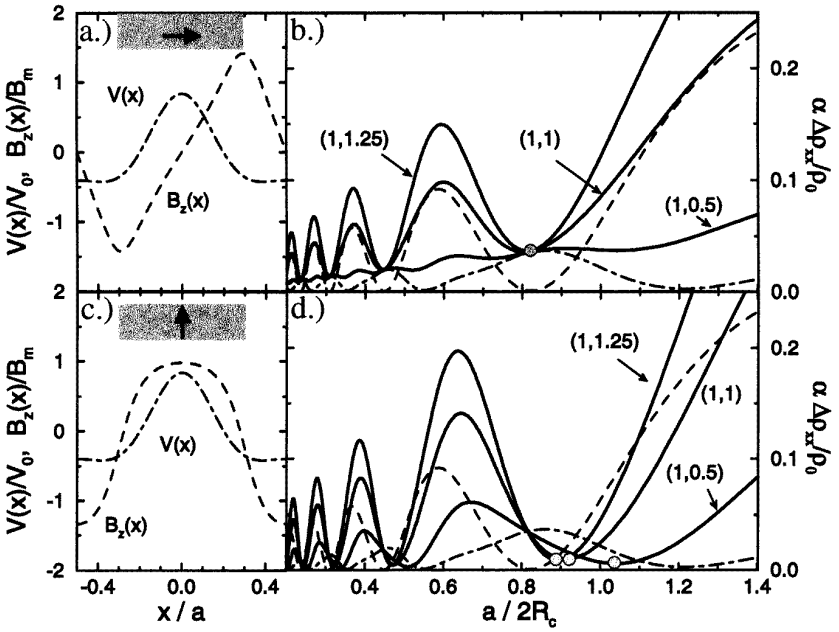

Figure 5. Left panel: normalized electric (dash-dotted) and magnetic (dashed) modulation fields calculated for a 1D lattice (period a) of strips of width $0.6a$ and height $0.4a$ magnetized either in the x (a) or in the z direction (c). The insets mark the positions and magnetization directions of the strips. The corresponding normalized and scaled (see [15]) magnetoresistance traces are shown in the right panels, where the dash-dotted curves refer to purely electric modulation, i.e. $(\epsilon, \mu) = (1, 0)$ and the dashed curves to purely magnetic modulation $(\epsilon, \mu) = (0, 1)$. The solid curves are calculated for a mixed modulation with the indicated (ϵ, μ) values.

phase shift, already addressed in [8], has consequences: while a magnetization in the z direction leads to real Fourier coefficients, that is to a pure cosine expansion of the modulation magnetic field, the magnetization in the x direction leads to purely imaginary coefficients, i.e. a sine expansion. As a result the Landau bands no longer become flat since now magnetic and electric modulation are simply added, $|s_m|^2 + |s_e|^2$. This additive behaviour can clearly be seen in the traces of figure 4 where the strips are magnetized parallel to the 2DEG. The dashed trace is taken directly after cooling down the device and the oscillations in ρ_{xx} are perfectly described by a pure electrostatic periodic potential, strain-imposed upon the 2DEG. With increasing B^{max} the effect of the magnetic field modulation takes over, as can be seen from the minima position at the magnetic flat-band condition (full triangles). At the magnetic flat-band condition $\lambda = 1$ near $B_0 \sim 0.28$ T it is obvious that the ρ_{xx} minimum 'sits' upon the maximum originating from the electric modulation.

Figure 5 displays calculations [15] illustrating the characteristic features observed in experiment. Figures 5(a) and 5(c) show the phase relation between the strain-induced potential $V_m(x)$ and the magnetic stray field $B_m(x)$. In figures 5(b) and 5(d) dashed and dash-dotted ρ_{xx} traces are calculated for pure magnetic and electric modulation, respectively. The solid curves are obtained for different normalized strengths μ of the magnetic modulation relative to a fixed electric modulation $\epsilon = 1$ (for a detailed description of the calculations and the definitions see [15]). For the in-phase situation in figure 5(d) the positions of the minima shift, as in experiment, when the amplitude of the stray field is increased (from $\mu = 0.5$ to 1.25) from the electric flat-band condition at $a/2R_c \sim 1.3$ to the magnetic one at $a/2R_c \sim 0.8$ (corresponding to $B_0 < 0$ in figure 3). In contrast, for out-of-phase modulations the ρ_{xx} traces at magnetic flat-band conditions in figure 5(b) all meet in one point on top of the electric-modulation-induced ρ_{xx} maxima.

Acknowledgments

We gratefully acknowledge technical support by M Riek, B Schönherr and U Waizmann. The work was supported by the German Bundesministerium für Bildung und Forschung (BMBF).

References

[1] Ye P D, Weiss D, Gerhardts R R, Seeger M, von Klitzing K, Eberl K and Nickel H 1995 *Phys. Rev. Lett.* **74** 3013
[2] Izawa S, Katsumoto S, Endo A and Iye Y 1995 *J. Phys. Soc. Japan* **64** 706
[3] Carmona H A, Geim A K, Nogaret A, Main P C, Foster T J, Henini M, Beaumont S P and Blamire M G 1995 *Phys. Rev. Lett.* **74** 3009
[4] Ye P D, Weiss D, von Klitzing K, Eberl K and Nickel H 1995 *Appl. Phys. Lett.* **67** 1441
[5] Ye P D *et al* unpublished. The influence of random magnetic fields on magnetotransport has been studied previously also by means of 'rough' macroscopic magnets:

Mancoff F B, Clarke R M, Marcus C M, Zhang S C, Campman K and Gossard A C 1995 *Phys. Rev.* B **51** 13 269; or by using stochastically distributed vortices in a type-II superconducting film. See, e.g.,
Bending S J, von Klitzing K and Ploog K 1990 *Phys. Rev. Lett.* **65** 1060
Geim A K, Bending S J, Grigorieva I V and Blamire M G 1994 *Phys. Rev.* B **49** 5749
[6] Davies J H and Larkin I A 1994 *Phys. Rev.* B **49** 4800
[7] Vasilopoulos P and Peeters F M 1990 *Superlatt. Microstruct.* **7** 393
[8] Peeters F M and Vasilopoulos P 1993 *Phys. Rev.* B **47** 1466
[9] Xue D P and Xiao G 1992 *Phys. Rev.* B **45** 5986
[10] Yagi R and Iye Y 1993 *J. Phys. Soc. Japan* **62** 1279
[11] Weiss D, von Klitzing K, Ploog K and Weimann G 1989 *Europhys. Lett.* **8** 179
See also *High Magnetic Fields in Semiconductor Physics II (Springer Series in Solid State Sciences 87)* ed G Landwehr (Berlin: Springer) p 357
[12] Gerhardts R R, Weiss D and von Klitzing K 1989 *Phys. Rev. Lett.* **62** 1173
[13] Winkler R W, Kotthaus J P and Ploog K 1989 *Phys. Rev. Lett.* **62** 1177
[14] Beenakker C W J 1989 *Phys. Rev. Lett.* **62** 2020
[15] Gerhardts R R 1996 *Phys. Rev.* B **53** at press